ARMY RESEARCH LABORATORY

120-mm Gun Tube Erosion Including Surface Chemistry Effects

by P. J. Conroy,
P. Weinacht, and M. J. Nusca

ARL-TR-1526

October 1997

The findings in this report are not to be construed as an official Department of the Army position unless so designated by other authorized documents.

Citation of manufacturer's or trade names does not constitute an official endorsement or approval of the use thereof.

Destroy this report when it is no longer needed. Do not return it to the originator.

Army Research Laboratory
Aberdeen Proving Ground, MD 21005-5066

ARL-TR-1526 October 1997

120-mm Gun Tube Erosion Including Surface Chemistry Effects

P. J. Conroy, P. Weinacht, M. J. Nusca
Weapons and Materials Research Directorate, ARL

Abstract

A theoretical model that addresses thermochemical erosion in gun tubes is presented. The model incorporates two interior ballistics codes—XKTC and IBHVG2—and the thermochemical code BLAKE to provide the necessary state variables and bulk species concentrations of the core flow as input. This erosion model utilizes a Crank-Nicolson integration scheme, with dynamic gridding capability to account for material ablation, as well as the addition of energy sources and heat transfer augmentation due to surface deviations. A mass transport scheme, utilizing the Lennard Jones 6-12 diffusion model, enables individual species to be transported to the surface from the core flow. Also fully coupled is a separate thermochemical routine which incorporates the NASA Lewis database. The code is written modularly, enabling the inclusion and modification of existing submodules. Erosion results comparing a fielded kinetic energy tank round and a candidate next-generation tank round are presented. The thermochemical effects at the surface are also shown and discussed.

Table of Contents

INTENTIONALLY LEFT BLANK.

List of Figures

List of Tables

INTENTIONALLY LEFT BLANK.

1. Introduction

Gun tubes are typically either erosion or fatigue limited in the number of rounds that can be effectively and safely fired from them. Direct-fire weapons are typically erosion-life limited due to the high-performance requirements placed upon them. Ammunition for the M256 tank gun is designed to maximize the kinetic energy of the projectile at launch. New performance requirements have reintroduced gun bore erosion as a significant design issue because erosion will limit the number of rounds that can be effectively and safely fired over the life of the gun tube. Previous "solutions" had not identified the fundamental cause of the erosion, and some discrepancies between the flame temperature correlations [1, 2, 3] and the erosivity were never resolved. Attempts to model erosion using first principles have been and are currently being made [4, 5, 6], although it is believed that significant additional work is still required.

A complete description of the erosion process would include a variety of mechanisms produced by thermal, chemical, and mechanical effects. Generally, thermal erosion is driven by high convective heating produced by the propellant gases that heat the in-bore surface of the gun tube and cause it to melt. Chemical erosion is caused by surface chemical reactions produced by the interaction of the gun tube gases with the in-bore surface of the tube. These reactions may erode the in-bore surface directly through pyrolysis or produce additional heat to augment the convective heating, thus inducing melting. The thermal and chemical erosion mechanisms are common and generally interrelated, while erosion due to mechanical effects (projectile passage) is more isolated and somewhat independent. In this current work, we have focused on the coupled thermal and chemical erosion mechanisms, while not excluding the possible addition of the mechanical contribution in the future.

2. Model Description

The model description is composed of three fully coupled portions consisting of thermal ablation and heat transfer/conduction, mass transport, and the imbedded thermochemistry, as well as the intercoupling of these portions.

Following a modular engineering approach resulted in the integration of some of the U.S. Army Research Laboratory's (ARL) well-developed tools as well as the development of new modules to supply additional physics—namely, an interior ballistics code to provide the necessary state variables and gas velocities XKTC [7], and a chemical equilibrium code BLAKE [8] coupled to an interior ballistic code, IBHVG2 [9] (thus creating the IBBLAKE [10] code, which provides temporal species concentrations), as well as the gun tube heat transfer-conduction code XBR-2D [11, 12, 13].

The current modeling effort considers a melt-wipe model similar to that proposed by Caveny [14], with the addition of surface chemistry. Conceptually, as shown in Figure 1, the surface heats from convection until the chemical activation energy is overcome; at this point a surface reaction occurs, releasing additional energy into the system and producing various products. The reaction products can either remain, as some solids, or be removed from the area as liquids or gases, thus resulting in ablation or pyrolysis, respectively. As the surface regresses, the solids are refreshed when the virgin substrate material is exposed. The following assumptions have been made in the model:

(1) One-dimensional (1-D) heat conduction is considered.

(2) No subsurface diffusion of species or reactions is considered.

(3) All surface liquids are removed.

(4) All surface gas products are removed.

(5) There is no feedback to the interior ballistics.

(6) Chemical energy released is treated as a source term.

(7) Species are chemically frozen from core flow to wall.

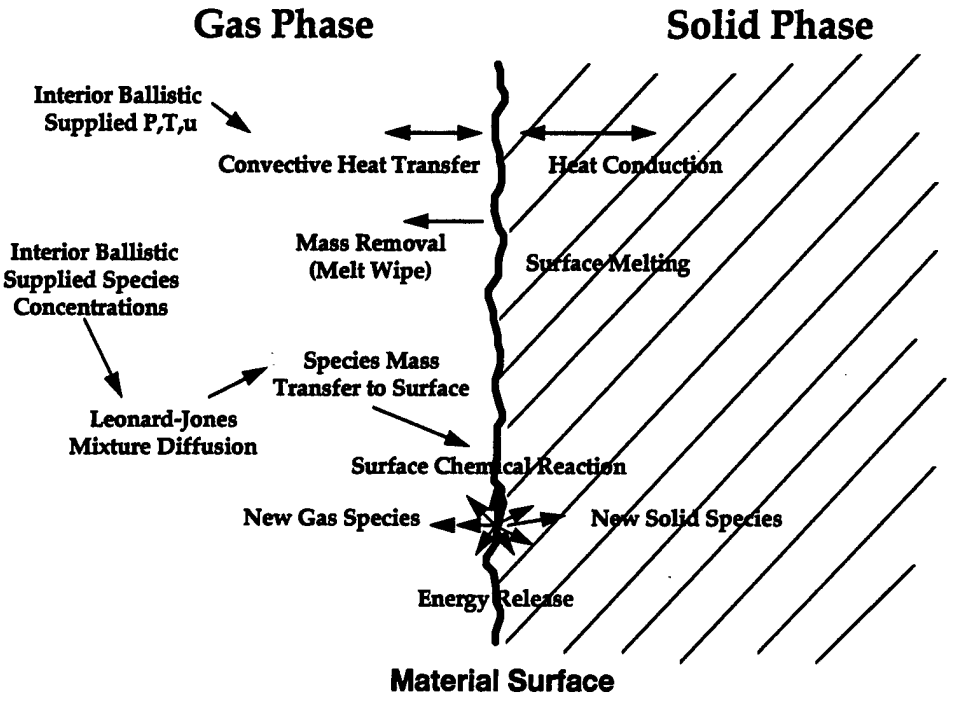

Figure 1. Conceptual Erosion Model.

3. Ablation-Conduction Model and Computational Approach

3.1 Analytical Description of the Ablation-Conduction Model [15]. The in-depth temperature response of the unablated (solid) material is modeled using 1-D heat conduction equation shown as follows:

$$\rho C_p \frac{\partial T}{\partial t} = \frac{1}{r^\beta} \frac{\partial}{\partial r} \left(r^\beta k \frac{\partial T}{\partial r} \right). \tag{1}$$

By setting $\beta = 0$ or $\beta = 1$, the planar or axisymmetric form of the governing equation can be obtained. In this form of the equation, the relevant material properties (density [ρ], specific heat [C_p], and conductivity [k]), the conductivity may vary, with all the others remaining continuous. The feature of variable conductivity was not utilized in the results presented here.

At the internal surface of the gun tube, two separate boundary conditions were applied depending on whether melting of the surface material was occurring. When the surface material was below the melt temperature, a convective heat transfer boundary condition was applied,

$$h\left(T_{gas} - T_{wall}\right) = -k\frac{\partial T}{\partial r} - Source, \tag{2}$$

with a source term due to the additional energy released from surface reactions. Using the state variables and gas velocity from the XKTC [7] code, the convective heat transfer coefficient, h, is determined using the correlation of Stratford and Beavers [16]. Once the surface of the gun tube reaches the melt temperature, melting of the surface material is assumed to occur. When fully molten (complete change of phase from solid to liquid), the liquid metal is immediately removed or ablated by the shearing action of the gun gases. Because surface material is being removed during the ablation process, the surface location (or the regression rate) becomes an additional variable. During the ablation process, two boundary conditions are applied as follows:

$$T_{wall} = T_{melt}$$

$$-k\frac{\partial T}{\partial r} = h\left(T_{gas} - T_{wall}\right) - \rho L\frac{\partial s}{\partial t} + Source.$$

The first equality of the melting boundary condition simply states that the temperature at the interface, while the phase change is occurring, is equal to the melt temperature. The melt temperature is assumed to be a known material property. The second equality of the boundary condition is obtained from an energy balance at the melt surface. In addition to the heat transfer due to conduction and convection, the additional energy required due to the change of phase from solid to liquid (latent heat of melting, L) is also included. This boundary condition allows the regression rate of the solid material to be computed, given that the latent heat of melting, L, is a known material property.

To provide closure for the in-depth temperature response of the gun tube, a convective boundary condition is applied to the outer surface of the gun tube.

$$h_{amb}\left(T_{wall_o} - T_{\infty}\right) = -k\frac{\partial T}{\partial r}. \quad (3)$$

However, because the erosion process occurs during the first several milliseconds of the firing process, the heat can only penetrate a fraction of the distance from the inner surface of the gun tube to the outer surface of the gun tube. In this case, it may not be necessary to model the radial temperature response of the entire gun tube. By locating the outer edge of the computational domain so that the temperature response is unchanged during the heating process, a smaller computational domain may be analyzed. In this case, one of two boundary conditions may be applied—a constant temperature boundary condition or an adiabatic wall boundary condition.

The appropriate depth of the computational domain can be estimated using a depth of penetration analysis [17, 18]. The depth of penetration, δ, gives the approximate distance that the heat would penetrate in a given time t and is a function of the thermal diffusivity of the material, α.

$$\delta = \sqrt{12\ \alpha\ t}. \quad (4)$$

Using a factor of safety of two or three δ will place the outer boundary of the computational domain far enough from the bore surface of the gun tube so that the temperature at the outer boundary remains unaffected by the heating of the gun tube during firing. This analysis enables either single-firing or rapid, continuous-fire erosion prediction.

The governing equations and boundary conditions are solved using a Crank-Nicolson finite-difference technique. Prior to the onset of melting, the governing equations and boundary conditions are linear, and solutions are obtained in a direct (noniterative) fashion. During the melting process, the equations become nonlinear, since the dimensions of the computational domain are coupled with the regression rate. An iterative approach is utilized during melting to appropriately address the nonlinearity.

Because the boundary of the computational domain moves during the erosion event, a transformed version of the governing equation is employed. This allows the equations to be solved in a fixed computational space even though the physical boundary is moving. A generalized transformation between the computational coordinate, ξ, and the physical coordinate, r, is utilized. The transformed equations are shown as follows:

$$\rho C_p \left(\frac{\partial T}{\partial t} + \xi_t \frac{\partial T}{\partial \xi} \right) = \frac{1}{r} \xi_r \frac{\partial}{\partial \xi} \left(r k \xi_r \frac{\partial T}{\partial \xi} \right)$$

$$\xi_t = \frac{-r_t}{r_\xi} \equiv \frac{-\frac{\partial r}{\partial t}}{\frac{\partial r}{\partial \xi}}$$

$$\xi_r = \frac{1}{r_\xi} \equiv \frac{1}{\frac{\partial r}{\partial \xi}}.$$

In this form, the nonlinear nature of the governing equation produced by the moving boundary is evident because the metric terms, ξ_r and ξ_t, are not constant and are dependent on the erosion rate when the grid is moving.

3.2 Comparison of Ablation-Conduction Model With Semianalytical Approach of Landau (Without Source Term). Over the past several decades, numerous studies examining the phase change process have been made. Results from two of these studies have been compared with the current numerical method without the inclusion of surface chemistry for simplicity. Landau [19] has made 1-D time-dependent numerical predictions of a melting solid using a technique similar to that utilized here. Landau considered the case of a semi-infinite solid subject to a constant heat flux. Goodman [20] considered similar problems using a heat-balance integral approach that utilizes an assumed form of the temperature profile to analytically determine the heat conduction and ablation process. While exact solutions are not typically obtained, the results are reasonably accurate and are of a simple form. One of the cases addressed by Goodman was the melting of a semi-infinite solid under constant heat flux. In both cases, an ablative boundary condition was utilized; that is, the liquid phase was immediately removed following melting.

The problem of the heating on a semi-infinite solid subject to constant heat flux was addressed using the current numerical method. The solid initially had a uniform temperature distribution of T_o and a specified melt temperature, T_{melt}. The temperature change is normalized by $T_{melt} - T_o$, while the in-wall depth is normalized by $(t_{melt}\alpha)^{0.5}$. Figure 2 shows the in-depth temperature profile at several increments in time during the melting process. The results were obtained using material properties corresponding to gun steel. In addition to the numerical results, the analytical results obtained using the heat-balance integral approach of Goodman are also shown at the onset of melting and during steady-state melting. The numerical solution and the analytical results are in excellent agreement at the onset of melting. (Though not shown, both results are also in excellent agreement with the exact analytical solution.) As the melting progresses, the temperature gradient at the heated interface is reduced due to the additional energy required to melt the solid (latent heat of melting) as shown in equation 4 repeated here for clarity without the source term

$$\rho L \frac{\partial s}{\partial t} = h\left(T_{gas} - T_{wall}\right) + k\frac{\partial T}{\partial r}.$$

After approximately eight times the time required to reach the melt temperature, the numerical results show that temperature profile has nearly reached the steady-state temperature profile. The differences between the analytical and numerical steady-state temperature profile are less than 2% of the difference between the melt temperature and the initial temperature. Exact agreement between the two results is not expected because the assumed form of the temperature profile in the heat-balance integral approach is not an exact solution.

A comparison of the predicted ablation rate obtained using the current technique with the results of Landau is shown in Figure 3. The current results are in excellent agreement with the results of Landau for three different sets of material properties including properties close to gun steel, m = 2.26 in Figure 3. (Differences between the results of Landau and the current result may be more related to problems in extracting the data from the original published graphs of Landau than to numerical

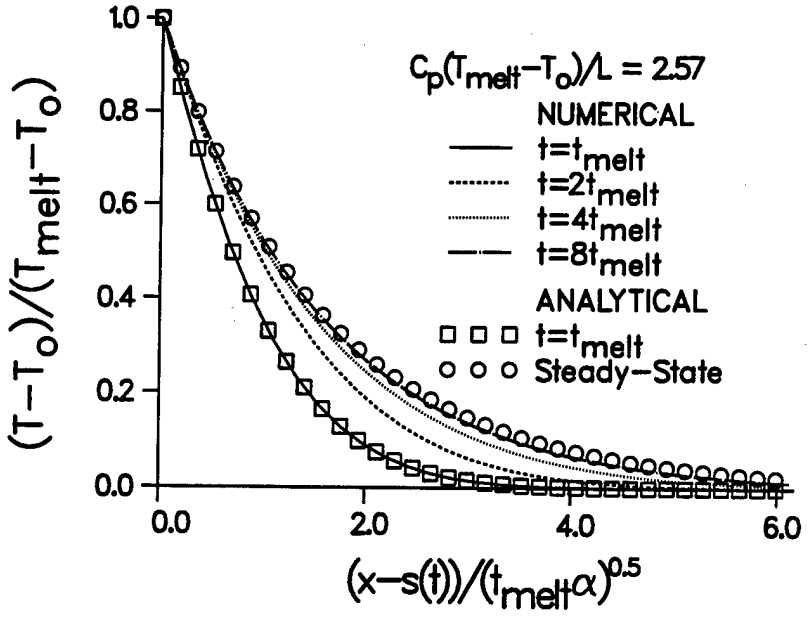

Figure 2. In-Depth Temperature Profile During Ablation Process for a Semi-Infinite Slab Subject to Constant Heat Flux.

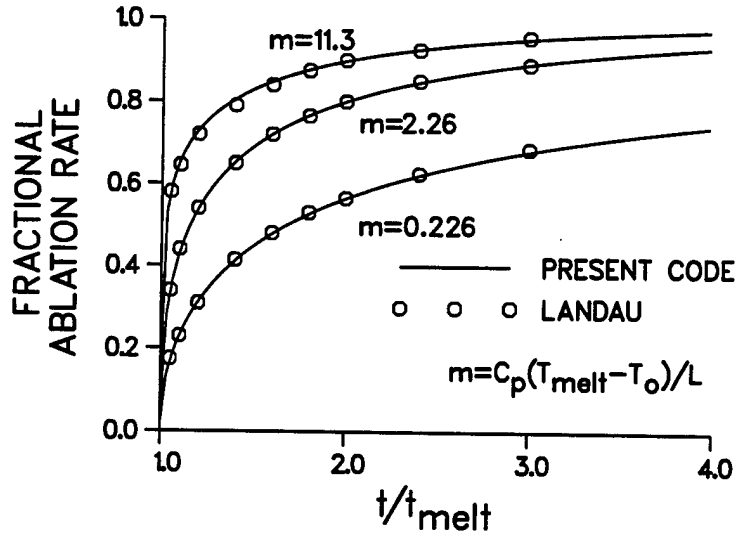

Figure 3. Fractional Ablation Rate vs. Time for a Semi-Infinite Slab Subject to Constant Heat Flux (m ≈ 2.26 for Gun Steel).

accuracy.) The steady-state ablation rate for the current result is also in good agreement with the exact analytical results presented by Landau.

Up to this point in the report, the convective energy transport, heat conduction, and surface melt wipe model have been developed. The following section 4 deals with the transport of the mass from the core flow (center of the bore/chamber) to the wall through the turbulent boundary layer. The species transported to the surface will then be reacted with the surface through a procedure outlined in section 5.

4. Mass Transport and Multicomponent Diffusion

The mass transport is modeled using mass transport coefficients not unlike the heat transport coefficient. However, because each species may diffuse differently due to its molecular weight, the proportions at the wall may be different than in the core flow. This requires each species to be transported individually to the wall through the mixture. Mass transport coefficients are represented in Sherwood number correlations ($Sh \equiv h_m L/D_{AB}$), as h_m, where L is a length parameter, and the diffusion coefficient, $D_{AB,}$ must also be determined.

A general outline of the mass transport procedure is as follows:

(1) Determine the binary diffusion coefficient for each species using the Lennard Jones potential parameters.

(2) Determine the mixture diffusion coefficient and viscosity for each specie through Wilke's mixing rule.

(3) Determine the mass transport coefficient from the Sherwood correlations.

(4) Solve the boundary condition for each species, similarly to the energy transport.

4.1 Section 1. A reasonable representation of binary diffusion of species "1" into species "2" is provided by the following relationship using the Lennard Jones 6-12 potential function parameters [21]:

$$D_{12} = \frac{0.0026280\sqrt{T^3(M_1 + M_2)/2M_1M_2}}{P\sigma_{12}^2\,\Omega_{12}^{(1,1)*}\left(T_{12}^*\right)}, \tag{5}$$

where M_1, M_2 are the molecular weights of the species, T is temperature, P is pressure, and, σ_{12}'s are the collision diameters for low-energy collisions. The collisional cross-section integral quantities, Ω^*_{12}'s, are obtained through table interpolation. The potential function for a particular species "i" governing the Lennard Jones model [21] is presented as

$$\Psi_i(r) = 4\epsilon_i\left[\left(\frac{\sigma_i}{r_i}\right)^{12} - \left(\frac{\sigma_i}{r_i}\right)^{6}\right], \tag{6}$$

where ϵ_i is the depth of the potential well. The potential well depths, ϵ_i's, and the collisional diameters, σ_i's, are provided in tabulated form for various species.

The following nondimensional temperature T_{12}^* is used as a tabulation parameter for the Lennard-Jones collisional cross section, Ω^*_{12}, integrals, where k is the Boltzmans constant,

$$T_{12}^* = \frac{Tk}{\epsilon_{12}}. \tag{7}$$

Combinatory analysis [21] is needed as shown to correctly apply the tabulated single species values in equation 6 and nondimensionalize the temperature in equation 7.

$$\epsilon_{12} = \sqrt{\epsilon_1\epsilon_2}, \qquad \sigma_{12} = \frac{(\sigma_1 + \sigma_2)}{2}.$$

4.2 Section 2. The computed binary diffusion provides the basis for the multicomponent diffusion coefficient. Each binary diffusion possibility is used and weighted vs. all other possibilities in the following mixture coefficient combinatory function [22].

$$D_{im} = \frac{1 - X_i}{\sum_{j \neq i} \frac{X_j}{D_{ij}}}.$$

where X_i is the mass fraction of series. This function enables the calculation of the diffusion coefficient for a particular specie "*i*" into a mixture "*m*" of many species. Equilibrium calculations for all service propellants were performed, and all principle products species σ's and k/ϵ's along with the collisional cross sections, $\Omega(T^*)$, were placed into data statements in the diffusion routine. Thus, tracking of an individual species contribution to the erosion process is possible. The aforementioned methodology was independently checked against known diffusivities with good agreement.

Utilizing the collisional cross sections, Ω_μ's, for viscocity and collisional diameters, σ's, and the molecular weight, the following relationship derived from kinetic theory [21] is utilized to determine the mixture viscocity using Wilke's rule. The mixture viscosity is used in developing the Reynolds number and Schmidt number, $Sc = \mu/\rho D_{AB}$, where ρ is the density.

$$\mu = 2.6693 \times 10^{-5} \frac{\sqrt{MT}}{\sigma^2 \Omega_\mu}.$$

4.3 Section 3. The development of the mass transport coefficients may now proceed with the previously developed computational methodology for both the diffusion coefficients and viscosities of the species in the mixture.

Mass transport to the surface from the core flow is provided through a species concentration potential ($\phi_{i\ core\ flow} - \phi_{i\ wall}$) and a mass transport coefficient, h_m, for each species. The species concentration of the core flow is provided by IBBLAKE [10] while the species concentration at the surface "wall" is what is being sought.

Development of appropriate Sherwood number correlations requires boundary layer analysis and experimental data. Mass transport for a transient boundary layer development as shown in Figure 4 has been derived [23] and will be presented here for a periodic transitional sublayer boundary layer model that assumes infrequent penetration to the surface (thin wall layer) by eddies entering the boundary layer. This approach enables predictions of transfer rates matching experimental data over a wide range of Schmidt numbers. The thin laminar wall layer beneath the boundary layer is periodically replenished with species from the sublayer, however at a much slower rate than the bulk wall region. The importance of the thin wall layer determines the treatment of the model.

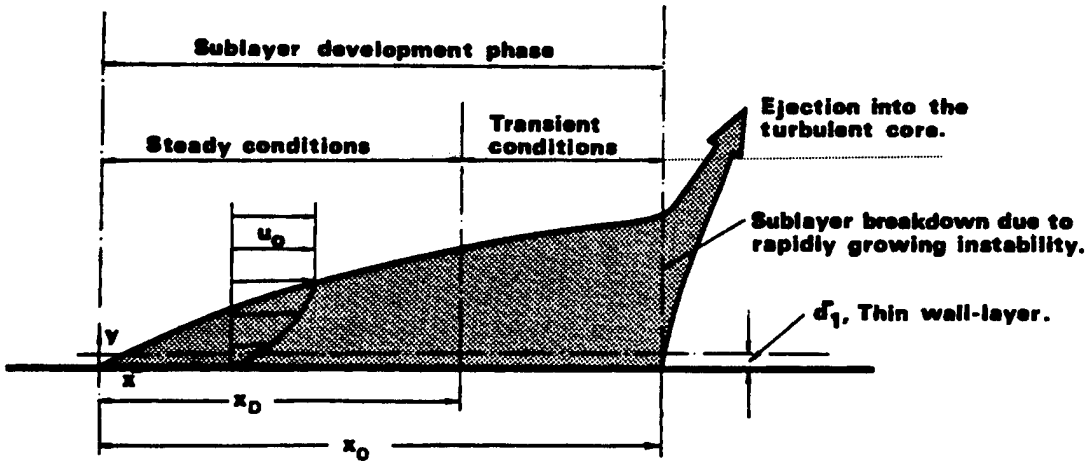

Figure 4. Idealized Boundary Layer Development [23].

At moderate Schmidt numbers ($10 < Sc < 1{,}000$), the thickness of the boundary layer is much greater than the thickness of the viscous sublayer. This enables the accumulation in the wall layer to be neglected. Ruckenstein [24] assumed the following linear pressure gradient model to govern the mass transport to the surface through the thin wall layer

$$\dot{m} = \frac{k}{\delta_1}\left(P_0 - P_1\right),$$

where k is the conductivity and δ_1 is the thickness of the thin wall layer. Utilizing the momentum integral method [23], the following Sherwood number has been derived:

$$Sh = \frac{0.0097 Re^{\frac{9}{10}} Sc^{\frac{1}{2}} \left(1.10 + 0.44 Sc^{-\frac{1}{3}} - 0.70 Sc^{-\frac{1}{6}}\right)}{1 + 0.064 Sc^{\frac{1}{2}} \left(1.10 + 0.44 Sc^{-\frac{1}{3}} - 0.70 Sc^{-\frac{1}{6}}\right)}.$$

For higher Schmidt numbers ($Sc > 1{,}000$) the thickness of the boundary layer becomes of the order of magnitude of the thin wall layer. The mass transport for this range is governed by the penetration of eddies into the boundary layer, in this case the wall layer [23]. This description, assuming characteristic distances between eddy disruptions is larger in the wall layer than it is in the boundary layer and Blasius expression for the friction factor, leads to the following Sherwood number:

$$Sh = 0.0102 Re^{\frac{9}{10}} Sc^{\frac{1}{3}}.$$

These expressions for the Sherwood number have been compared [23] with much experimental data and agree very well within the Schmidt number regions specified.

4.4 Section 4. The Sherwood number values and appropriate diffusivities enable the calculation of the mass transport coefficient that closes the boundary condition. The mass transport coefficients, h_m's, are derived from Sherwood number correlations, $Sh \equiv h_m L/D_{im}$, and integrated over space and time, as shown, to provide the temporally varying species at the surface.

$$Mass_i = \int\int h_m \left(\phi_{icore\text{-}flow} - \phi_{iwall}\right) dA\, dt.$$

Although the gaseous species are assumed to not penetrate the surface at this time, the diffusion module is general enough to readily incorporate this possibility in the future.

At this point, both the convective energy transport and mass transport have been presented. Thus, the state properties as well as surface concentrations of specific species have been described. At this point, some treatment of the solid-gaseous interaction can be made. Due to the lack of understanding of both the specific surface reactions and rates associated with these reactions under ballistic conditions, infinite rate kinetics have been applied in this model as a first approximation to the surface chemistry. A brief description of the energy minimization methodology for equilibrium reactions follows.

5. Equilibrium Kinetics

Equilibrium chemical processes are considered to dominate whenever the characteristic time for a "fluid element" (discritized element in finite difference model of a continuum region of a fluid dynamic event) to traverse the "flow field of interest" (a fluid dynamic event) is much longer than the characteristic time for chemical reactions to approach equilibrium. As the pressure and temperature increase, the molecular collision frequency and energy per collision increase, which leads to smaller characteristic chemical times. Thus, chemical processes approach equilibrium (i.e., occur at almost an infinite rate).

Chemical equilibrium is usually described by either of two equivalent formulations: equilibrium constants or minimization of free energy. Several disadvantages of the equilibrium constant method have been noted [25], and most researchers prefer the free-energy minimization formulation. The condition for equilibrium may be stated in terms of any of several thermodynamic functions such as the minimization of the Gibbs free energy or Helmholtz free energy or the maximization of entropy. For a mixture of N species (e.g., atoms or molecules) with the number of moles of species denoted n_i, the Gibbs energy per mole of mixture is given in terms of the Gibbs free energy of the individual

species, g_i, the internal energy, e, the temperature, T, the entropy, s, the pressure, p, and the specific volume, V.

$$G = \sum_{i=1}^{N} n_i g_i = e - Ts + pV.$$

The equilibrium method employed in the present study is based on the fact that at equilibrium the total Gibbs energy of the system attains a minimum value. The problem is to find the set of n_i's that minimizes the Gibbs free energy for a specified energy and volume (e,V), subject to the constraints of material balances. The standard solution to this type of problem is based on the method of Lagrange's undetermined multipliers. First, we must recognize that the total number of atoms of each element in the system is constant. Denoting a particular atomic species with subscript k, then A_k is the total number of atomic masses of the kth element in the system, as determined by the initial constitution of the system. Denoting the number of atoms of the kth element present in each molecule of chemical species i by a_{ik}, then the material balance on each element k may be written (M used here is the number of elements),

$$\sum_{k=1}^{M} \lambda_k \left(\sum_{i=1}^{N} n_i a_{ik} - A_k \right) = 0 \qquad (k = 1, 2, ..., M) \tag{8}$$

introducing Lagrange multipliers, λ_k, for each element. Then a new function, F, is formed by addition of the last equation to G_{total}. The function F is identical to G_{total} since the summation term is zero. However, $\partial F/\partial n_i$ and $\partial G_{total}/\partial n_i$ are different since F incorporates the constraints of the material balances. The minimum of both F and G_{total} occurs when these partial derivatives are zero.

$$F = G_{total} + \sum_{k=1}^{M} \lambda_k \left(\sum_{i=1}^{N} n_i a_{ik} - A_k \right)$$

$$\left(\frac{\partial F}{\partial n_i} \right)_{e,V,n_i} = \left(\frac{\partial G_{total}}{\partial n_i} \right)_{e,V,n_i} + \sum_{k=1}^{M} \lambda_k a_{ik} = 0 \qquad (\textit{for } F_{\min}).$$

This equation can be rewritten using the definition of chemical potential α_i, for species i, where R_u is the universal gas constant.

$$\delta_i = \left(\frac{\partial G_{total}}{\partial n_i} \right)_{e,V,n_i} = G_i^o + R_u T \ln (\alpha_i),$$

$$\delta_i + \sum_{k=1}^{M} \lambda_k a_{ik} = 0 \qquad (i = 1,2,...,N). \tag{9}$$

The standard Gibbs-energy change of formation for species i is denoted G_i^o, which is equal to zero for elements in their standard states. The activity for species i in solution is given by α_i, defined in terms of the equilibrium constant K as

$$K = \prod_i^N \alpha_i^{\nu_i},$$

where the activities of the components are raised to the corresponding stoichiometric coefficients, ν_i. For an ideal gas mixture ($X_i \phi_i = 1$), where ϕ_i is the void fraction,

$$\alpha_i = f_i = X_i \phi_i p = p,$$

f_i is the fugacity and X_i is the mole fraction for the ith species. For liquids and solid phases,

$$\ln (\alpha_i) = \ln (1 - 1/p),$$

which is approximately zero for large pressure; therefore, $\delta_i = G^o$.

There are N equilibrium equations (equation 9), one for each species, and there are M material-balance equations (equation 8), one for each element, a total of $N + M$ equations. The unknowns in these equations are the n_i's, of which there are N, and the λ_k's, of which there are M, a total of $N + M$. Thus, the number of equations is sufficient for the determination of all unknowns.

Numerical experiments were performed on this portion of the code as well to independently verify reaction calculations results from this routine with known results. Principally, known gas phase systems were investigated. The results of which compared exactly with those of the NASA-Lewis equilibrium code [25].

6. Surface Erosion Results

Due to current development programs, the first application of the coupled ablation-chemical surface reaction model has been directed toward direct-fire systems. The model is used to compare the relative erosion performance in the M256 cannon firing the M829A1 KE projectile and an advanced KE projectile concept round. Both of these rounds are built from similar propellants, although the flame temperature of the M829A1 propellant is lower than that of the advanced concept. The thermal performance of the M829A1 KE round has been investigated previously [26] with excellent agreement between the model and existing experimental data, as was the case with numerous previous applications [12, 13].

The ARL erosion code calculations require a core flow thermochemical output from IBBLAKE, and an XKTC output file including the spatially varying gas pressure, temperature, and velocity [27]. For both calculations, the barrel was assumed not to have a chrome layer. Once degraded, the chrome's effectiveness is small [28]. It will be seen that this assumption possibly has some validity for the advanced KE round, while for the less viscerative M829A1 round this assumption appears to be somewhat excessive.

Results of the calculations are shown in Figures 5–10. Figures 5 and 6 show surface temperature predictions for both the M829A1 and the advanced round at three representative axial locations, 640 m, 1,050 mm, and 1,350 mm from the rear face of the tube (RFT). The 640-mm location is near the forcing cone region. One can see from Figure 5 that the surface just reaches the specified melt temperature at the 640-mm axial location, while at the more distant locations down-bore, the surface does not reach the melt temperature. Experimentally, bore erosion has been observed at both the

640-mm and the 1,050-mm locations, but not at the 1,350-mm locations in tubes having fired the M829A1 round [28]. Looking at Figure 6, what is first noticed is that the melting in this case is much more severe and for a much longer duration at all three axial locations predicted. Also noted is that the peak temperature for this round is reached somewhat later and longer in duration than that of the M829A1. This is due to the different propellant grain geometry, which was designed to create just such an effect in the pressure profile, in order to optimize the ballistic performance with the given constraints.

The erosion for the M829A1 round is typically located near the forcing cone at 640 mm. However, erosion has been observed initiating somewhat down-bore at the 1,050-mm location in some guns. This "abnormal" erosion pattern is under investigation and is believed to be due somewhat to the interaction of the forward bore rider with the tube, in a scraping, or perhaps the aluminum bore rider is reacting with existing atmospheric oxygen in the tube forward of the projectile [28]. This would increase the rate of chrome removal at these specific locations and thus expose the underlying bare steel.

Figures 7 and 8 show the predicted resultant surface heat fluxes due to convection and thermochemical reactions. Notice that in both cases the level of thermochemical energy imparted to the surface is on the order of 1% of the total energy. This is intuitively correct because convective heat transfer calculations gave very good agreement with experimental data [26]. The M829A1 flux rises and decays much more rapidly than that of the advanced round, again due to the charge design. The advanced round shows a spike at the peak of the flux that is believed to be caused by the "slivering" (the point at which the grain burns through its web) of the grain.

Predicted erosion rates are shown in Figure 9 for both rounds. The erosion rate for the M829A1 is almost an order of magnitude smaller than that of the advanced round. Even though the surface temperature is constant during melting, the erosion rate follows the heat flux contour, including the spike at the peak heating rate. The erosion rate decreases for the advanced round as the axial location increases from the RFT.

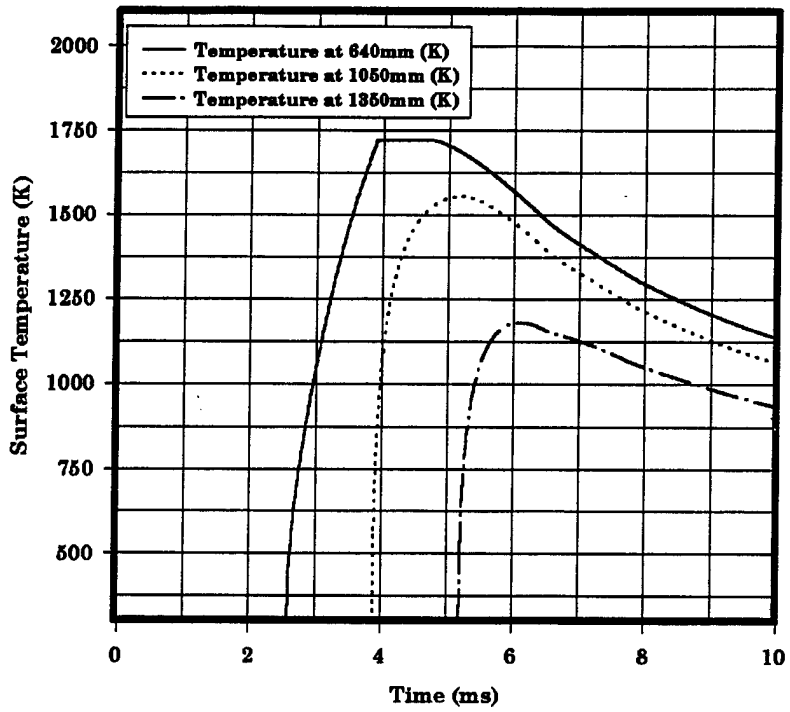

Figure 5. Predicted Surface Temperatures for the M829A1 KE Round in a Nonchromed M256 Cannon.

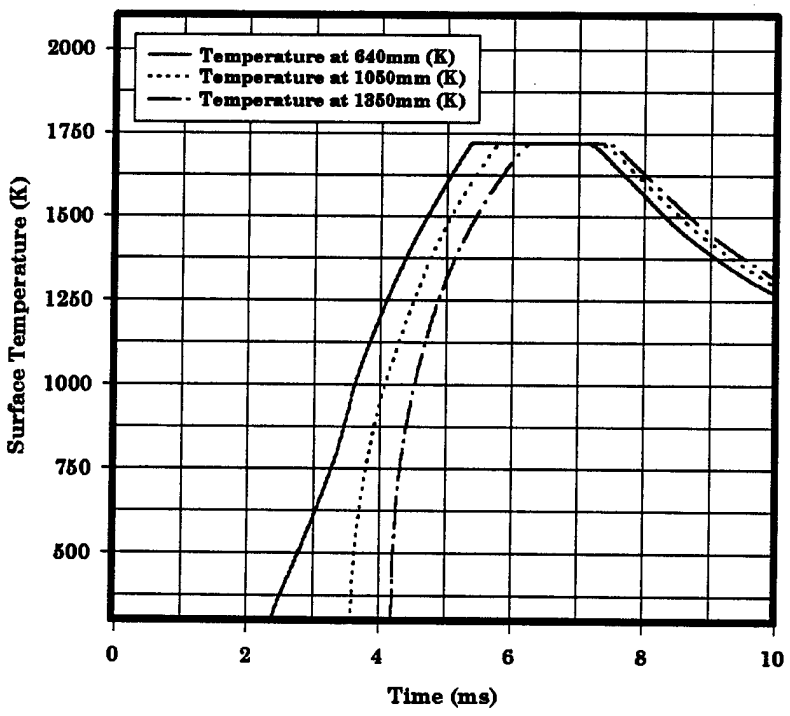

Figure 6. Predicted Surface Temperatures for an Advanced KE Round in a Nonchromed M256 Cannon.

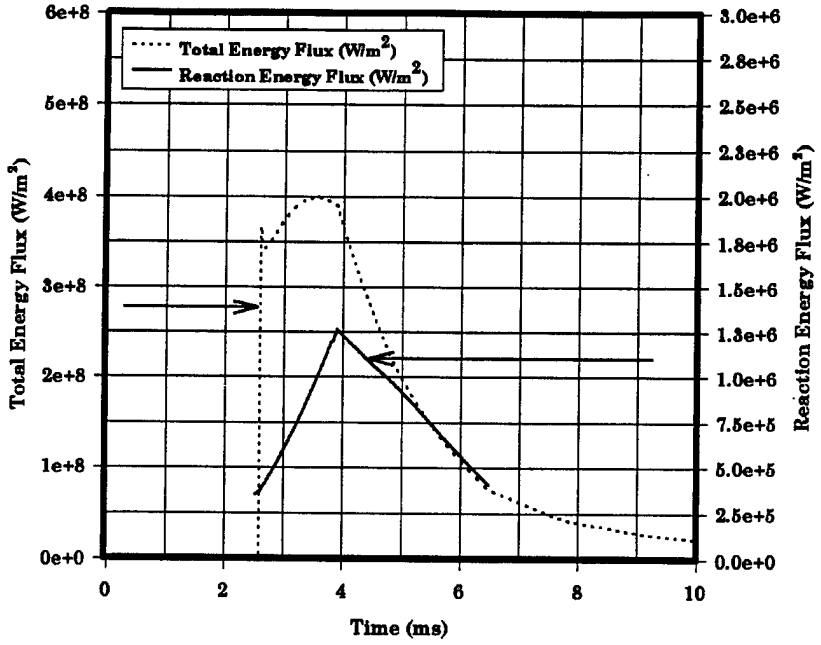

Figure 7. Predicted Energy Flux Distribution at 0.64 m From RFT for an M829A1 KE Round in a Nonchromed M256 Cannon.

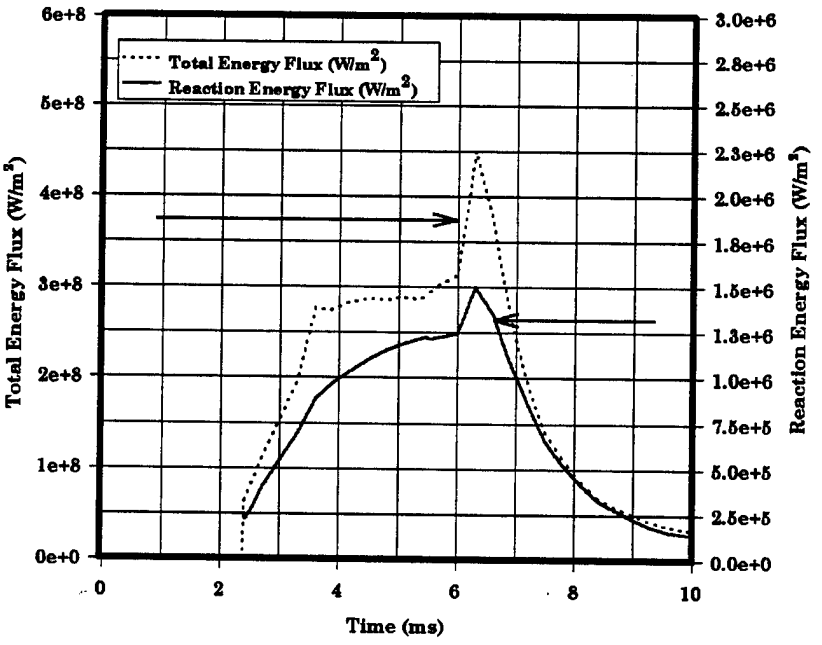

Figure 8. Predicted Energy Flux Distribution at 0.64 m From RFT for an Advanced KE Round in a Nonchromed M256 Cannon.

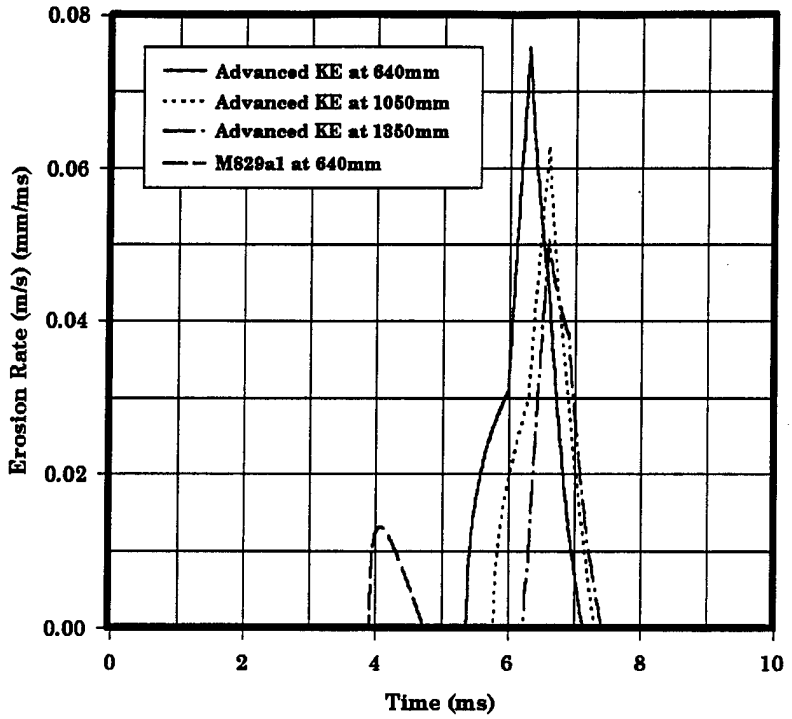

Figure 9. Predicted Erosion Rates for an Advanced KE Penetrator at Three Axial Locations and the Erosion Rate for an M829A1 KE Penetrator at One Axial Location.

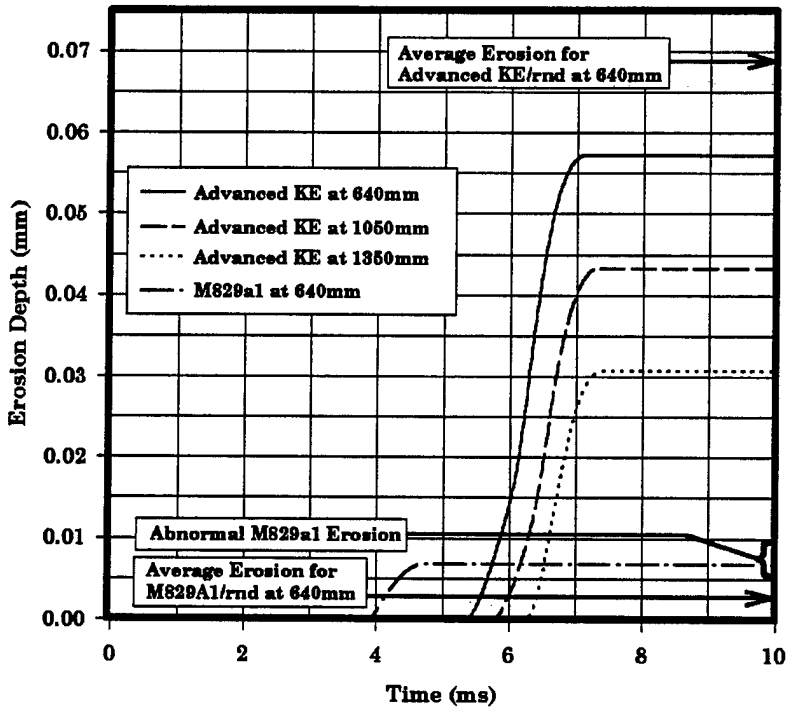

Figure 10. Predicted Erosion Depths per Round for an Advanced KE Penetrator at Three Locations and the Erosion Depth per Round for an M829A1 KE Penetrator at One Axial Location. Also Presented Is Averaged Experimental Erosion Depths per Round for Both Penetrators.

Figure 10 reveals the amount of material removed per round fired, for both rounds. The M829A1 erodes much less at the forcing cone region than the advanced round. The predicted erosion is about 16% below the experimental data (average of 39 rounds) for the advanced round and a bit high for the average M829A1 round. For the "abnormal" erosion described previously, the M829A1 calculations were within the data range. The use of constant physical properties in the calculations probably accounted for some of this discrepancy [28, 29]. It is also possible that for the M829A1 rounds more chrome existed at the surface near the forcing cone, thus inhibiting the erosion.

7. Surface Chemistry Results

Table 1 is representative of the chemistry occurring at the surface, at a specific location, during the peak surface temperature time step. Both the unreacted (input) and reacted (output) species from the thermochemical calculation are presented. A total of 34 species were considered for both the M829A1 and advanced KE penetrator, although many of the potential product species were not formed. A user may choose any material for the surface or any additional gas products from the propellant combustion. For these calculations O_2, CO_2, H_2, CO, H_2O, N_2, SO_2, and NO represented about 98% of the combustion products. The surface was considered to be steel consisting of Fe(A),* Cr_2O_3, NI(B), and C(GR).† The following species were included in all of the thermochemical calculations; however, they converged to a value within an internally specified tolerance on the mass fraction for zero: NI, NIO, NO_2, HNO, HCO RAD, CRO, CRO_2, SO, COS, S_2 , FEO(S),§ FEO(L),** FE, FEO, FEO_2H_2, FE(L), FE_3O_4(S), OH, OH+, and S.

The preliminary equilibrium chemistry results from both rounds were basically the same because of the similar propellant formulation. Due to the chemical equilibrium assumption and the affinity for CO_2 formation, carbon and oxygen are formed from the "apparent breakdown" of the CO_2 reactant at the surface. The molecular oxygen reacts with the molecular hydrogen to make water, while the carbon forms graphite. The added FE(A) goes through the phase transition to FE(C),‡ and the additional NI(B) melts. During this time step and at this location, the surface is regressing and is being replenished with fresh "steel." The CR_2O_3 in the steel acts inertly, as does the N_2 from the

---

* A - Base-centered cubic; † GR - Carbon graphite; § S - Solid; ** L - Liquid; ‡ C - Face-centered cubic.

Table 1. Representative Chemical Reactants and Products During Melting of the Surface

Time (ms) = 5.349	Energy Released (J/kg) = 12218.7			
	Unreacted Species at the Surface (Input)		Reaction Products at the Surface (Output)	
Species	Mass (kg)	Fraction	Mass (kg)	Fraction
H_2	0.4553E-06	0.1147E-01	0.8000E-20	0.2016E-15
O_2	0.9061E-13	0.2283E-08	0.1270E-18	0.3200E-14
CO	0.7709E-05	0.1943E+00	0.9855E-05	0.2483E+00
CO_2	0.6656E-05	0.1677E+00	0.1747E-18	0.4401E-14
H_2O	0.3950E-05	0.9953E-01	0.8019E-05	0.2021E+00
SO_2	0.0000E+00	0.0000E+00	0.2542E-18	0.6406E-14
N_2	0.1073E-05	0.2704E-01	0.1073E-05	0.2704E-01
NO	0.2222E-11	0.5599E-07	0.1191E-18	0.3001E-14
C(GR)	0.8020E-07	0.2021E-02	0.9766E-06	0.2461E-01
FE(A)	0.1759E-07	0.4432E-03	0.2216E-18	0.5585E-14
NI(B)	0.3299E-09	0.8313E-05	0.2330E-18	0.5870E-14
$CR_2O_3(S)$	0.1634E-06	0.4117E-02	0.1634E-06	0.4117E-02
FE(C)	0.1958E-04	0.4934E+00	0.1960E-04	0.4939E+00
NI(L)	0.0000E+00	0.0000E+00	0.3299E-09	0.8313E-05
	Total Mass (kg) 0.3969E-04		Total Mass (kg) 0.3969E-04	
	Before Sum of Mass Fractions = 0.1000E+01		After Sum of Mass Fractions = 0.1000E+01	

gas. One interesting point is that the graphite formed may create a physical property modification if it dissolves or diffuses into the surface of the steel.

8. Discussion

A numerical method for estimating the erosion that occurs within gun tubes due to high convective and chemically reactive in-bore heating has been developed. The method has been successfully applied to estimate the erosion that may occur during the firing of M829A1 and advanced kinetic energy projectiles fired from an M256 cannon that has the chrome chipped away. While chrome is present, the surface does not reach a high enough temperature to enable the chrome nor the substrate to melt. If the surface is gun steel (i.e., the chrome has chipped off), then the predicted levels of erosion are roughly in agreement with experimental observations at the forcing cone. The prediction for the M829A1 is probably high due to the absence of chrome in the model, while the computed values for the advanced KE round were a bit low, possibly reinforcing the assumption that the chrome was not very effective in protecting the surface. With the addition of currently excluded physics, such as surface layers, surface defects, gas intrusion, species diffusion, and in-wall altered material properties, the predictions should improve.

The current model provides the U.S. Army with the ability to predict the effects of modifications to the propelling charge and to the chemical propulsion technique (i.e., liquid or solid propellants). It is evident that small chemical formulation changes greatly alter the erosion behavior [30]. Tracking these chemical modifications and their impact on the erosion behavior is now possible. This tool may be especially useful in estimating the erosive behavior before the development of new charges. It is intended to be used as a platform to build upon to include the mechanical portion of the erosion and to investigate other physics of interest such as the effect of wear-reducing additives and surface treatments. Potentially, newer and more direct mitigation techniques may be identified once the causality of a specific erosion problem is determined. Also, this model has been written to incorporate boundary conditions from future interior ballistic codes such as NGEN [31]. NGEN will be fully turbulent, enabling the turbulent reacting boundary layer to be computed. This coupling will strengthen the mass and heat transfer physics and enable more confidence in the solutions.

9. References

1. "Proceedings of the Interservice Technical Meeting on: Gun Tube Erosion and Control." Watervliet Arsenal, Watervliet, NY, 25–26 February 1970.

2. "Proceedings of the Tri-Service Gun Tube Wear and Erosion Symposium." U.S. Army Armament Research Development and Engineering Center, Dover, NJ, 29–31 March 1977.

3. Lawton, Brian. "Thermal and Chemical Effects on Gun Barrel Wear." Proceedings of the 8th International Symposium on Ballistics, Orlando, FL, 23–25 October 1984.

4. Evans, Michael R. "User's Manual for Transient Boundary Layer Integral Matrix Procedure TBLIMP." Aerotherm UM-74-55, Prepared for Naval Ordnance Station, Indian Head, MD, October 1974.

5. Dunn, Stuart, et al. "Unified Computer Model for Predicting Thermochemical Erosion in Gun Barrels." AIAA 95-2440, July 1995.

6. Conroy, P. J., P. Weinacht, and M. J. Nusca. "U.S. Army Research Laboratory Tube Erosion Code (ATEC)." *Proceedings of the 32nd JANNAF Combustion Subcommittee Meeting*, October 1995.

7. Gough, Paul S. "The XNOVAKTC Code." BRL-CR-627, U.S. Army Ballistic Research Laboratory, Aberdeen Proving Ground, MD, February 1990.

8. Freedman, Eli. "BLAKE - A Thermodynamic Code Based on Tiger: Users' Guide and Manual." BRL-TR-02411, U.S. Army Ballistic Research Laboratory, Aberdeen Proving Ground, MD, July 1982.

9. Anderson, Ronald D., and K. D. Fickie. "IBHVG2 - A Users Guide." BRL-TR-2829, U.S. Army Ballistic Research Laboratory, Aberdeen Proving Ground, MD, July 1987.

10. Janke, P. J., et al. "Electrothermo-Chemical Propellant Extensions to the IBHVG2 Interior Ballistics Simulation: Model Development and Validation." *Proceedings of the 31st JANNAF Combustion Meeting*, October 1994.

11. Crickenberger, Andrew B., Robert L. Talley, and James Q. Talley. "Modifications to the XBR-2D Heat Conduction Code." ARL-CR-126, U.S. Army Research Laboratory, Aberdeen Proving Ground, MD, April 1994.

12. Conroy, Paul J. "Gun Tube Heating." BRL-TR-3300, U.S. Army Ballistic Research Laboratory, Aberdeen Proving Ground, MD, December 1991.

13. Keller, George E., Paul J. Conroy, Terence P. Coffee, and J. Barns. "Chamber Heating of the AFAS Gun." ARL-TR-799, U.S. Army Research Laboratory, Aberdeen Proving Ground, MD, July 1995.

14. Caveny, Leonard H. "Steel Erosion Produced by Double Base, Triple Base, and RDX Composite Propellants of Various Flame Temperatures." ARLCD-CR-80016, U.S. Army Armament Research and Development Command, October 1980.

15. Weinacht, P., and P. J. Conroy. "A Numerical Method for Predicting Thermal Erosion in Gun Tubes." ARL-TR-1156, U.S. Army Research Laboratory, Aberdeen Proving Ground, MD, July 1996.

16. Stratford, B. S., and G. S. Beavers. "The Calculation of the Compressible Turbulent Boundary Layer in Arbitrary Pressure Gradient - A Correlation of Certain Previous Methods." Aeronautical Research Council R\&M, No. 3207, Royal Armament Research and Development, United Kingdom, 1961.

17. Kakac, S., and Y. Yener. *Heat Conduction.* 2nd edition, New York: Hemisphere Publishing Co., 1985.

18. Özişik, M. N. *Heat Conduction.* New York: John Wiley and Sons, Inc., 1980.

19. Landau, H. G. "Heating Conduction in a Melting Solid." *Quarterly of Applied Mathematics*, vol. 8, pp. 81–94, 1950.

20. Goodman, T. R. "The Heat-Balance Integral and Its Application to Problems Involving a Change of Phase." *Transactions of the ASME*, vol. 80, pp. 335–342, 1958.

21. Hirschfelder, Curtis Bird. *Molecular Theory of Gases and Liquids.* New York: John Wiley and Sons Inc., March 1964.

22. Anderson, J. D. *Hypersonic + High Temperature Gas Dynamics.* New York: McGraw Hill, 1989.

23. Gutfinger, Chaim. *Topics in Transport Phenomena.* New York: John Wiley and Sons, 1975.

24. Ruckenstein, E. "Some Remarks on Renewal Models." Chemical Engineering Science, vol. 18, pp. 223, 1963.

25. Gordon, S., and B. J. McBride. "Computer Program for Calculation of Complex Chemical Equilibrium Compositions, Rocket Performance, Incident and Reflected Shocks, and Chapman-Jouget Detonations." NASA SP-273, NASA Lewis, OH, 1971.

26. Conroy, P. J., M. Bundy, and J. Kennedy. "Simulated and Experimental In-Wall Temperatures for 120-mm Ammunition." ARL-TR-770, U.S. Army Research Laboratory, Aberdeen Proving Ground, MD, June 1995.

27. Mr. Andrew Brant of the ARL was instrumental in providing the necessary XKTC, BLAKE, and IBHVG2 databases for the conceptual advanced KE round, March 1996.

28. Gerber, N., and M. Bundy. "Effect of Variable Thermal Properties on Gun Tube Heating." BRL-MR-3984, U.S. Army Ballistic Research Laboratory, Aberdeen Proving Ground, MD, July 1992.

29. Bundy, M. L., N. Gerber, and J. W. Bradley. "Evaluating Potential Bore Melting From Firing M829A1 Ammunition." ARL-MR-107, U.S. Army Research Laboratory, Aberdeen Proving Ground, MD, October 1993.

30. Downs, David S., et al. "Prediction of Wear Characteristics of Artillery Propelling Charges." ARDEC-TR-80016, Large Caliber Weapon Systems Lab, Dover, NJ, March 1981. AD-E400572.

31. Nusca, Michael J. "Investigation of Solid Propellant Gun Systems Using the Next-Generation Interior Ballistics Code." *Proceedings of the 31st JANNAF Combustion Meeting*, CPIA Publication no. 620, vol. 1, pp. 279–292, October 1994.

INTENTIONALLY LEFT BLANK.

NO. OF COPIES	ORGANIZATION
2	DEFENSE TECHNICAL INFORMATION CENTER DTIC DDA 8725 JOHN J KINGMAN RD STE 0944 FT BELVOIR VA 22060-6218
1	HQDA DAMO FDQ DENNIS SCHMIDT 400 ARMY PENTAGON WASHINGTON DC 20310-0460
1	DPTY ASSIST SCY FOR R&T SARD TT F MILTON RM 3EA79 THE PENTAGON WASHINGTON DC 20310-0103
1	OSD OUSD(A&T)/ODDDR&E(R) J LUPO THE PENTAGON WASHINGTON DC 20301-7100
1	CECOM SP & TRRSTRL COMMCTN DIV AMSEL RD ST MC M H SOICHER FT MONMOUTH NJ 07703-5203
1	PRIN DPTY FOR TCHNLGY HQ US ARMY MATCOM AMCDCG T M FISETTE 5001 EISENHOWER AVE ALEXANDRIA VA 22333-0001
1	PRIN DPTY FOR ACQUSTN HQS US ARMY MATCOM AMCDCG A D ADAMS 5001 EISENHOWER AVE ALEXANDRIA VA 22333-0001
1	DPTY CG FOR RDE HQS US ARMY MATCOM AMCRD BG BEAUCHAMP 5001 EISENHOWER AVE ALEXANDRIA VA 22333-0001

NO. OF COPIES	ORGANIZATION
1	INST FOR ADVNCD TCHNLGY THE UNIV OF TEXAS AT AUSTIN PO BOX 202797 AUSTIN TX 78720-2797
1	USAASA MOAS AI W PARRON 9325 GUNSTON RD STE N319 FT BELVOIR VA 22060-5582
1	CECOM PM GPS COL S YOUNG FT MONMOUTH NJ 07703
1	GPS JOINT PROG OFC DIR COL J CLAY 2435 VELA WAY STE 1613 LOS ANGELES AFB CA 90245-5500
1	ELECTRONIC SYS DIV DIR CECOM RDEC J NIEMELA FT MONMOUTH NJ 07703
3	DARPA L STOTTS J PENNELLA B KASPAR 3701 N FAIRFAX DR ARLINGTON VA 22203-1714
1	USAF SMC/CED DMA/JPO M ISON 2435 VELA WAY STE 1613 LOS ANGELES AFB CA 90245-5500
1	US MILITARY ACADEMY MATH SCI CTR OF EXCELLENCE DEPT OF MATHEMATICAL SCI MDN A MAJ DON ENGEN THAYER HALL WEST POINT NY 10996-1786
1	DIRECTOR US ARMY RESEARCH LAB AMSRL CS AL TP 2800 POWDER MILL RD ADELPHI MD 20783-1145

NO. OF
COPIES ORGANIZATION

1 DIRECTOR
US ARMY RESEARCH LAB
AMSRL CS AL TA
2800 POWDER MILL RD
ADELPHI MD 20783-1145

3 DIRECTOR
US ARMY RESEARCH LAB
AMSRL CI LL
2800 POWDER MILL RD
ADELPHI MD 20783-1145

ABERDEEN PROVING GROUND

4 DIR USARL
AMSRL CI LP (305)

NO. OF COPIES	ORGANIZATION
1	HQDA SARD TR MS K KOMINOS PENTAGON WASHINGTON DC 20310-0103
1	HQDA SARD TR DR R CHAIT PENTAGON WASHINGTON DC 20310-0103
1	CHAIRMAN DOD EXPLOSIVES SAFETY BD HOFFMAN BLDG 1 RM 856 C 2461 EISENHOWER AVE ALEXANDRIA VA 22331-0600
1	HQS US ARMY MATERIEL CMD AMCICP AD M FISETTTE 5001 EISENHOWER AVE ALEXANDRIA VA 22333-0001
1	US ARMY BMDS CMD ADVANCED TECHLGY CTR PO BOX 1500 HUNTSVILLE AL 35807-3801
1	OFC OF THE PRODUCT MGR SFAE AR HIP IP R DE KLEINE 155MM HOWITZER M109A6 PALADIN PICATINNY ARSENAL NJ 07806-5000
3	PM ADV FIELD ARTLRY SYS SFAE ASM AF E LTC A ELLIS T KURIATA J SHIELDS PICATINNY ARSENAL NJ 07801-5000
1	PM ADV FIELD ARTLRY SYSTEM SFAE ASM AF Q W WARREN PICATINNY ARSENAL NJ 07801-5000

NO. OF COPIES	ORGANIZATION
1	CDR US ARMY ARDEC PROD BASE MODERNIZATION AGENCY AMSMC PBM A SIKLOSI PICATINNY ARSENAL NJ 07806-5000
1	CDR US ARMY ARDEC PROD BASE MODRNZTN AGENCY AMSMC PBM E L LAIBSON PICATINNY ARSENAL NJ 07806-5000
1	PM PEO ARMAMENTS TANK MAIN ARMAMENT SYS AMCPM TMA PICATINNY ARSENAL NJ 07806-5000
1	PM PEO ARMAMENTS TANK MAIN ARMAMENT SYS AMCPM TMA 105 PICATINNY ARSENAL NJ 07806-5000
1	PM PEO ARMAMENTS TANK MAIN ARMAMENT SYS AMCPM TMA 120 PICATINNY ARSENAL NJ 07806-5000
1	PM PEO ARMAMENTS TANK MAIN ARMAMENT SYSTEM AMCPM TMA AS H YUEN PICATINNY ARSENAL NJ 07806-5000
2	CDR US ARMY ARDEC AMSTA AR CCH V C MANDALA E FENNELL PICATINNY ARSENAL NJ 07806-5000
1	CDR US ARMY ARDEC AMSTA AR CCH T L ROSENDORF PICATINNY ARSENAL NJ 07806-5000

NO. OF COPIES	ORGANIZATION
1	CDR US ARMY ARDEC AMSTA AR CCS PICATINNY ARSENAL NJ 07806-5000
1	CDR US ARMY ARDEC AMSTA AR AEE J LANNON PICATINNY ARSENAL NJ 07806-5000
10	CDR US ARMY ARDEC AMSTA AR AEE B D DOWNS S EINSTEIN S WESTLEY S BERNSTEIN J RUTKOWSKI B BRODMAN P O'REILLY R CIRINCIONE P HUI J O'REILLY PICATINNY ARSENAL NJ 07806-5000
5	CDR US ARMY ARDEC AMSTA AR AEE WW M MEZGER J PINTO D WIEGAND P LU C CHU PICATINNY ARSENAL NJ 07806-5000
1	CDR US ARMY ARDEC AMSTA AR AES S KAPLOWITZ PICATINNY ARSENAL NJ 07806-5000
1	CDR US ARMY ARDEC AMSTA AR HFM E BARRIERES PICATINNY ARSENAL NJ 07806-5000
1	CDR US ARMY ARDEC AMSTA AR FSA T M SALSBURY PICATINNY ARSENAL NJ 07806-5000
1	CDR US ARMY ARDEC AMSTA AR FSA F LTC R RIDDLE PICATINNY ARSENAL NJ 07806-5000
1	CDR US ARMY ARDEC AMSTA AR FSC G FERDINAND PICATINNY ARSENAL NJ 07806-5000
1	COMMANDER AMSTA AR FS T GORA PICATINNY ARSENAL NJ 07806-5000
1	CDR US ARMY ARDEC AMSTA AR FS DH J FENECK PICATINNY ARSENAL NJ 07806-5000
3	CDR US ARMY ARDEC AMSTA AR FSS A R KOPMANN B MACHEK L PINDER PICATINNY ARSENAL NJ 07806-5000
1	CDR US ARMY ARDEC AMSTA AR FSN N K CHUNG PICATINNY ARSENAL NJ 07806-5000
2	DIR BENET WEAPONS LABS AMSTA AR CCB RA G P O'HARA G A PFLEGL WATERVLIET NY 12189-4050

NO. OF COPIES	ORGANIZATION
1	DIR BENET WEAPONS LABS AMSTA AR CCB RT S SOPOK WATERVLIET NY 12189-4050
1	DIR BENET WEAPONS LABS AMSTA AR CCB S F HEISER WATERVLIET NY 12189-4050
2	CDR US ARMY RSRCH OFC TECH LIB D MANN PO BOX 12211 RESEARCH TRIANGLE PARK NC 27709-2211
1	CDR USACECOM R&D TECH LIB ASQNC ELC IS L R MYER CTR FORT MONMOUTH NJ 07703-5301
1	CMDT USA AVIATION SCHL AVIATION AGENCY FORT RUCKER AL 36360
1	PM US TANK AUTOMOTIVE CMD AMCPM ABMS T DEAN WARREN MI 48092-2498
1	PM US TANK AUTOMOTIVE CMD FIGHTING VEHICLE SYSTEMS SFAE ASM BV WARREN MI 48397-5000
1	PM ABRAMS TANK SYSTEM SFAE ASM AB WARREN MI 48397-5000
1	DIR HQ TRAC RPD ATCD MA FORT MONROE VA 23651-5143
1	COMMANDER US ARMY BELVOIR R&D CTR STRBE WC FORT BELVOIR VA 22060-5006

NO. OF COPIES	ORGANIZATION
1	DIRECTOR US ARMY TRAC FORT LEE ATRC L MR CAMERON FORT LEE VA 23801-6140
1	COMMANDANT US ARMY CMD & GEN STAFF COLLEGE FORT LEAVENWORTH KS 66027
1	COMMANDANT USA SPECIAL WARFARE SCHL REV AND TRNG LIT DIV FORT BRAGG NC 28307
1	COMMANDER RADFORD ARMY AMMUNITION PLANT SMCAR QA HI LIB RADFORD VA 24141-0298
1	COMMANDER US ARMY NGIC AMXST MC 3 220 SEVENTH STREET NE CHARLOTTESVILLE VA 22901-5396
1	COMMANDANT USAFAC&S ATSF CD COL T STRICKLIN FORT SILL OK 73503-5600
1	COMMANDANT USAFC&S ATSF CN P GROSS FORT SILL OK 73503-5600
1	CMDT USA ARMOR SCHL ARMOR AGENCY ATZK CD MS M FALKOVITCH FORT KNOX KY 40121-5215
2	CDR NAVAL SEA SYSTEMS CMD SEA 62R SEA 64 WASHINGTON DC 20362-5101

NO. OF COPIES	ORGANIZATION
1	CDR NAVAL AIR SYSTEMS CMD AIR 954 TECH LIBRARY WASHINGTON DC 20360
4	CDR NAVAL RSRCH LAB TECH LIBRARY CODE 4410 K KAILASANATE J BORIS E ORAN WASHINGTON DC 20375-5000
1	OFFICE OF NAVAL RSRCH CODE 473 R S MILLER 800 N QUINCY ST ARLINGTON VA 22217-9999
1	OFFICE OF NAVAL TECHLGY ONT 213 D SIEGEL 800 N QUINCY ST ARLINGTON VA 22217-5000
1	CDR NAVAL SURFACE WARFARE CTR CODE 730 SILVER SPRING MD 20903-5000
1	CDR NAVAL SURFACE WARFARE CTR CODE R 13 R BERNECKER SILVER SPRING MD 20903-5000
7	CDR NAVAL SURFACE WARFARE CTR T C SMITH K RICE S MITCHELL S PETERS J CONSAGA C GOTZMER TECH LIB INDIAN HEAD MD 20640-5000
1	CDR NAVAL SURFACE WARFARE CTR CODE G30 GUNS & MUNITIONS DIV DAHLGREN VA 22448-5000

NO. OF COPIES	ORGANIZATION
1	CDR NAVAL SURFACE WARFARE CTR CODE G32 GUNS SYSTEMS DIV DAHLGREN VA 22448-5000
1	CDR NAVAL SURFACE WARFARE CTR CODE G33 T DORAN DAHLGREN VA 22448-5000
1	CDR NAVAL SURFACE WARFARE CTR CODE E23 TECH LIB DAHLGREN VA 22448-5000
2	CDR NAVAL AIR WARFARE CTR CODE 388 C F PRICE T BOGGS CHINA LAKE CA 93555-6001
2	CDR NAVAL AIR WARFARE CTR CODE 3895 T PARR R DERR CHINA LAKE CA 93555-6001
1	CDR NAVAL AIR WARFARE CTR INFORMATION SCIENCE DIV CHINA LAKE CA 93555-6001
1	COMMANDER OFFICER CODE 5B331 TECH LIB NAVAL UNDERWATER SYS CTR NEWPORT RI 02840
1	AFOSR NA J TISHKOFF BOLLING AFB DC 20332-6448
1	OLAC PL TSTL D SHIPLETT EDWARDS AFB CA 93523-5000

NO. OF COPIES	ORGANIZATION
3	AL LSCF J LEVINE L QUINN T EDWARDS EDWARDS AFB CA 93523-5000
1	WL MNAA B SIMPSON EGLIN AFB FL 32542-5434
1	WL MNME ENERGETTC MATERIALS BR 2306 PERIMETER RD STE 9 EGLIN AFB FL 32542-5910
1	WL MNSH R DRABCZUK EGLIN AFB FL 32542-5434
2	NASA LANGLEY RSRCH CTR M S 408 W SCALLION D WITCOFSKI HAMPTON VA 23605
1	CIA OFC OF THE CTR REFERENCES DISSEMINATION BR RM GE 47 HQS WASHINGTON DC 20502
1	CIA J BACKOFEN NHB RM 5N01 WASHINGTON DC 20505
1	SDIO TNI L H CAVENY PENTAGON WASHINGTON DC 20301-7100
1	SDIO DA E GERRY PENTAGON WASHINGTON DC 21301-7100

NO. OF COPIES	ORGANIZATION
2	HQ DNA D LEWIS A FAHEY 6801 TELEGRAPH RD ALEXANDRIA VA 22310-3398
1	DIR SANDIA NATL LABS M BAER DEPT 1512 PO BOX 5800 ALBUQUERQUE NM 87185
1	DIR SANDIA NATL LABS R CARLING COMBUSTION RSRCH FACILITY LIVERMORE CA 94551-0469
1	DIR SANDIA NATL LABS 8741 G A BENEDITTI PO BOX 969 LIVERMORE CA 94551-0969
2	DIR LLNL L 355 A BUCKINGHAM M FINGER PO BOX 808 LIVERMORE CA 94550-0622
1	DIR LANL T3 D BUTLER PO BOX 1663 LOS ALAMOS NM 87544
1	DIR LANL M DIV B CRAIG PO BOX 1663 LOS ALAMOS NM 87544
2	BATTELLE TWSTIAC V LEVIN 505 KING AVE COLUMBUS OH 43201-2693
1	BATTELLE PNL M GARNICH PO BOX 999 RICHLAND WA 99352

NO. OF COPIES ORGANIZATION

1 THE UNIV OF AUSTIN TEXAS
INST FOR ADVANCED TECHLGY
T M KIEHNE
4030 2 W BRAKER LANE
AUSTIN TX 78759-5329

2 CPIA JHU
H J HOFFMAN
T CHRISTIAN
10630 LITTLE PATUXENT PKWY
STE 202
COLUMBIA MD 21044-3200

1 AFELM THE RAND CORP
LIBRARY D
1700 MAIN ST
SANTA MONICA CA 90401-3297

1 BRIGHAM YOUNG UNIV
M BECKSTEAD
DEPT OF CHEMICAL ENGRG
PROVO UT 84601

1 CALIF INSTITUTE OF TECHLGY
L D STRAND MS 125 224
JET PROPULSION LAB
4800 OAK GROVE DR
PASADENA CA 91109

1 CALI INSTITUTE OF TECHLGY
F E C CULICK
204 KARMAN LAB
MAIN STOP 301 46
1201 E CALIFORNIA STR
PASADENA CA 91109

1 MILLERSVILLE UNIV
PHYSICS DEPT
C W PRICE
MILLERSVILLE PA 17551

3 GEORGIA INSTITUTE OF TECHLGY
SCHOOL OF AEROSPACE ENGRG
B T ZIM
E PRICE
W C STRAHLE
ATLANTA GA 30332

NO. OF COPIES ORGANIZATION

2 UNIV OF ILLINOIS
DEPT OF MECH INDUSTRY ENGRG
H KRIER
R BEDDINI
144 MEB 1206 N GREEN ST
URBANA IL 61801-2978

1 UNIV OF MASSACHUSETTS
DEPT OF MECHANICAL ENGRG
K JAKUS
AMHERST MA 01002-0014

1 UNIV OF MINNESOTA
DEPT OF MECHANICAL ENGRG
E FLETCHER
MINNEAPOLIS MN 55414-3368

4 PENNSYLVANIA STATE UNIV
DEPT OF MECHANICAL ENGRG
V YANG
K KUO
C MERKLE
G SETTLES
UNIVERSITY PARK PA 16802-7501

1 RENSSELAER POLYTECH INST
DEPT OF MATHEMATICS
TROY NY 12181

1 STEVENS INST OF TECHLGY
R MCALEVY III
DAVIDSON LAB
CASTLE POINT STATION
HOBOKEN NJ 07030-5907

1 RUTGERS UNIVERSITY
DEPT OF MECH AND AERO ENGRG
S TEMKIN
UNIV HEIGHTS CAMPUS
NEW BRUNSWICK NJ 08903

1 UNIV OF UTAH
DEPT OF CHEMICAL ENGRG
A BAER
SALT LAKE CITY UT 84112-1194

1 WASHNGTON STATE UNIV
DEPT OF MECHANICAL ENGRG
C T CROWE
PULLMAN WA 99163-5201

NO. OF COPIES	ORGANIZATION
1	ARROW TECHLGY ASSOC INC W HATHAWAY PO BOX 4218 SOUTH BURLINGTON VT 05401-0042
2	AAI CORPORANON J FRANKLE D CLEVELAND PO BOX 126 HUNT VALLEY MD 21030-0126
8	ALLIANT TECHSYSTEMS INC R E TOMPKINS J KENNEDY J BODE C CANDLAND L OSGOOD R BURETTA R BECKER M SWENSON 600 SECOND ST NE HOPKINS MN 55343
1	ELI FREEDMAN AND ASSOCIATES E FREEDMAN 2411 DIANA RD BALTIMORE MD 21209-1525
1	GENERAL APPLIED SCIENCES LAB J ERDOS 77 RAYNOR AVE RONKONKAMA NY 11779-6649
1	GENERAL ELECTRIC CO TACTICAL SYSTEM DEPT J MANDZY 100 PLASTICS AVE PITTSFIELD MA 01201-3698
1	IITRI M J KLEIN 10 W 35TH ST CHICAGO IL 60616-3799

NO. OF COPIES	ORGANIZATION
4	HERCULES INC L GIZZI D A WORRELL W J WORRELL C CHANDLER RADFORD ARMY AMMO PLANT RADFORD VA 24141-0299
2	HERCULES INC W B WALKUP T F FARABAUGH ALLEGHENY BALLISTICS LAB PO BOX 210 ROCKET CENTER WV 26726
1	HERCULES INC R CARTWRIGHT AEROSPACE 100 HOWARD BLVD KENVILLE NJ 07847
1	HERCULES INC B M RIGGLEMAN HERCULES PLAZA WILMINGTON DE 19894
1	MARTIN MARIETTA ARM SYS J TALLEY RM 1309 LAKESIDE AVE BURLINGTON VT 05401
1	MBR RESEARCH INC DR MOSHE BEN REUVEN 601 EWING STE C 22 PRINCETON NJ 08540
1	OLIN CORP F E WOLF BADGER ARMY AMMO PLANT BARABOO WI 53913
3	OLIN ORDNANCE E J KIRSCHKE A F GONZALEZ D W WORTHINGTON PO BOX 222 SAINT MARKS FL 32355-0222

NO. OF COPIES	ORGANIZATION
1	OLIN ORDNANCE H A MCELROY 10101 9TH ST NORTH SAINT PETERSBURG FL 33716
1	PAUL GOUGH ASSOC INC P S GOUGH 1048 SOUTH ST PORTSMOUTH NH 03801-5423
1	PHYSICS INTRNTNL LIB H WAYNE WAMPLER PO BOX 5010 SAN LEANDRO CA 94577-0599
1	PRINCETON CMBSTN RSRCH LABS INC A MESSINA PRINCETON CORPORATE PLAZA 11 DEERPARK DR BLDG IV STE 119 MONMOUTH JUNCTION NJ 08852
3	ROCKWELLINTRNTNL BA08 J FLANAGAN J GRAY R B EDELMAN ROCKETDYNE DIV 6633 CANOGA AVE CANOGA PARK CA 91303-2703
2	ROCKWELL INTRNTNL SCIENCE CTR DR S CHAKRAVARTHY DR S PALANISWAMY 1049 CAMINO DOS RIOS PO BOX 1085 THOUSAND OAKS CA 91360
1	SAIC M PALMER 2109 AIR PARK RD ALBUQUERQUE NM 87106
1	SOUTHWEST RSRCH INST J P RIEGEL 6220 CULEBRA RD PO DRAWER 28510 SAN ANTONIO TX 78228-0510
1	SVERDRUP TECHLGY INC DR JOHN DEUR 2001 AEROSPACE PARKWAY BROOK PARK OH 44142
3	THIOKOL CORP R WILLER R BIDDLE TECH LIB ELKTON DIV PO BOX 241 ELKTON MD 21921-0241
1	VERITAY TECHGY INC E FISHER A CRICKENBERGER J BARNES 4845 MILLERSPORT HWY EAST AMHERST NY 14501-0305
1	UNIVERSAL PROPULSION CO H J MCSPADDEN 25401 NORTH CENTRAL AVE PHOENIX AZ 85027-7837
1	SRI INTERNATIONAL TECH LIB PROPULSION SCIENCES DIV 333 RAVENWOOD AVE MENLO PARK CA 94025-3493

NO. OF COPIES	ORGANIZATION
	ABERDEEN PROVING GROUND
1	CDR USAATC STECS LI R HENDRICKSEN
34	DIR USARL AMSRL WM P A HORST AMSRL WM PA T MINOR T COFFEE G WREN A BIRK J DE SPIRITO A JUHASZ J KNAPTON C LEVERITT M MCQUAID W OBERLE P TRAN K WHITE L-M CHANG J COLBURN P CONROY G KELLER D KOOKER M NUSCA T ROSENBERGER AMSRL WM PB P PLOSTINS M BUNDY B GUIDOS D LYON J GARNER V OSKAY J SAHU P WEINACHT H EDGE E FERRY AMSRL WM PC B FORCH AMSRL WM PD B BURNS AMSRL SC C W STUREK C NIETUBICZ

INTENTIONALLY LEFT BLANK.

REPORT DOCUMENTATION PAGE

Form Approved
OMB No. 0704-0188

1. AGENCY USE ONLY *(Leave blank)*	2. REPORT DATE	3. REPORT TYPE AND DATES COVERED
	October 1997	Final, Jan 96 - Jan 97

4. TITLE AND SUBTITLE

120-mm Gun Tube Erosion Including Surface Chemistry Effects

5. FUNDING NUMBERS

1L162618AH80

6. AUTHOR(S)

P. J. Conroy, P. Weinacht, and M. J. Nusca

7. PERFORMING ORGANIZATION NAME(S) AND ADDRESS(ES)

U.S. Army Research Laboratory
ATTN: AMSRL-WM-PA
Aberdeen Proving Ground, MD 21005-5066

8. PERFORMING ORGANIZATION REPORT NUMBER

ARL-TR-1526

9. SPONSORING/MONITORING AGENCY NAMES(S) AND ADDRESS(ES)

10.SPONSORING/MONITORING AGENCY REPORT NUMBER

11. SUPPLEMENTARY NOTES

12a. DISTRIBUTION/AVAILABILITY STATEMENT

Approved for public release; distribution is unlimited.

12b. DISTRIBUTION CODE

13. ABSTRACT *(Maximum 200 words)*

A theoretical model that addresses thermochemical erosion in gun tubes is presented. The model incorporates two interior ballistics codes—XKTC and IBHVG2—and the thermochemical code BLAKE to provide the necessary state variables and bulk species concentrations of the core flow as input. This erosion model utilizes a Crank-Nicolson integration scheme, with dynamic gridding capability to account for material ablation, as well as the addition of energy sources and heat transfer augmentation due to surface deviations. A mass transport scheme, utilizing the Lennard Jones 6-12 diffusion model, enables individual species to be transported to the surface from the core flow. Also fully coupled is a separate thermochemical routine which incorporates the NASA Lewis database. The code is written modularly, enabling the inclusion and modification of existing submodules. Erosion results comparing a fielded kinetic energy tank round and a candidate next-generation tank round are presented. The thermochemical effects at the surface are also shown and discussed.

14. SUBJECT TERMS

erosion, gun tubes, surface chemistry

15. NUMBER OF PAGES

16. PRICE CODE

17. SECURITY CLASSIFICATION OF REPORT	18. SECURITY CLASSIFICATION OF THIS PAGE	19. SECURITY CLASSIFICATION OF ABSTRACT	20. LIMITATION OF ABSTRACT
UNCLASSIFIED	UNCLASSIFIED	UNCLASSIFIED	UL

INTENTIONALLY LEFT BLANK.

USER EVALUATION SHEET/CHANGE OF ADDRESS

This Laboratory undertakes a continuing effort to improve the quality of the reports it publishes. Your comments/answers to the items/questions below will aid us in our efforts.

1. ARL Report Number/Author ARL-TR-1526 (Conroy) Date of Report October 1997

2. Date Report Received _____

3. Does this report satisfy a need? (Comment on purpose, related project, or other area of interest for which the report will be used.) _____

4. Specifically, how is the report being used? (Information source, design data, procedure, source of ideas, etc.) _____

5. Has the information in this report led to any quantitative savings as far as man-hours or dollars saved, operating costs avoided, or efficiencies achieved, etc? If so, please elaborate. _____

6. General Comments. What do you think should be changed to improve future reports? (Indicate changes to organization, technical content, format, etc.) _____

CURRENT ADDRESS

Organization

Name E-mail Name

Street or P.O. Box No.

City, State, Zip Code

7. If indicating a Change of Address or Address Correction, please provide the Current or Correct address above and the Old or Incorrect address below.

OLD ADDRESS

Organization

Name

Street or P.O. Box No.

City, State, Zip Code

(Remove this sheet, fold as indicated, tape closed, and mail.)

(DO NOT STAPLE)

DEPARTMENT OF THE ARMY

OFFICIAL BUSINESS

NO POSTAGE
NECESSARY
IF MAILED
IN THE
UNITED STATES

BUSINESS REPLY MAIL
FIRST CLASS PERMIT NO 0001,APG,MD

POSTAGE WILL BE PAID BY ADDRESSEE

DIRECTOR
US ARMY RESEARCH LABORATORY
ATTN AMSRL WM PA
ABERDEEN PROVING GROUND MD 21005-5066